University of Pittsburgh

GPU-Accelerated Ray-Tracing Methods for Determining Radiation View Factors in Multi-Junction Thermoelectric Generators

Asher J. Hancock[1a] and:

Laura B. Fulton[2], Justin Ying[3], Shervin Sammak, Ph.D.[4], Matthew M. Barry, Ph.D[1]

[1]Department of Mechanical and Materials Science, UPitt

[2]School of Computer Science, CMU

[3]Department of Computer Engineering, UPitt

[4]Center for Research Computing, UPitt

ajh172@pitt.edu[a]

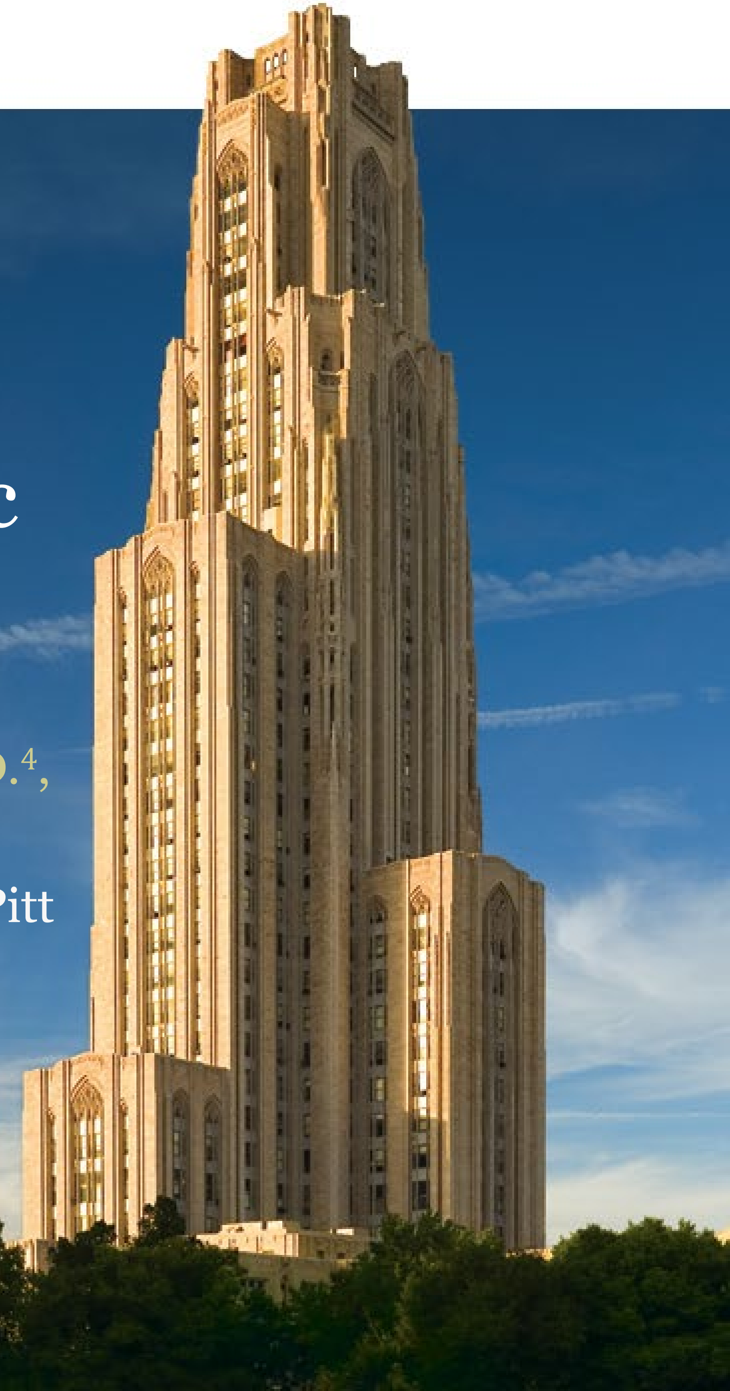

Background: Thermoelectric generators and uses

Thermoelectric generators (TEGs) are solid-state energy conversion devices

Show promise in space applications, as well as the automobile industries

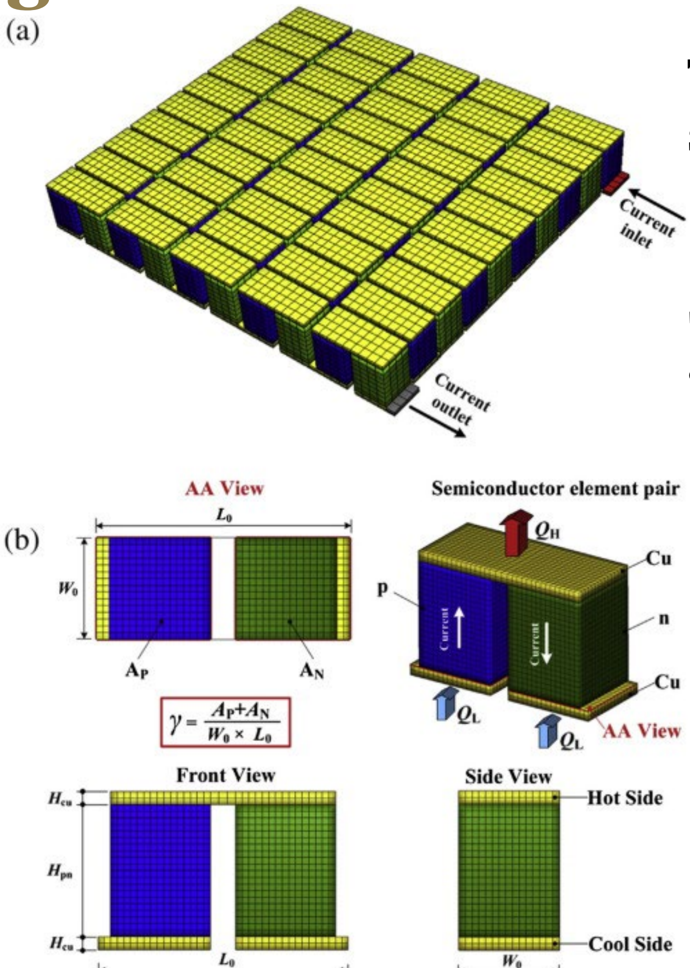

"Recent development and application of thermoelectric generator and cooler" (2015) in Applied Energy

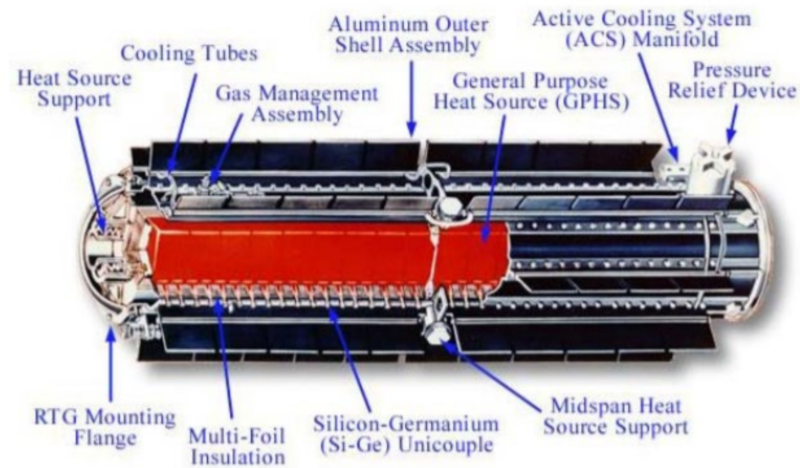

"US space radioisotope power systems and applications: past, present and future" (2011) in Radioisotopes-Applications in Physical Sciences

Outline:

Background: TEG design

Basics of a unit-cell thermoelectric generator design

- P- and N-type thermoelectric materials
- Conductive interconnectors (Int.)
- Heat source and heat sink
- String multiple cells together to form a TE modules

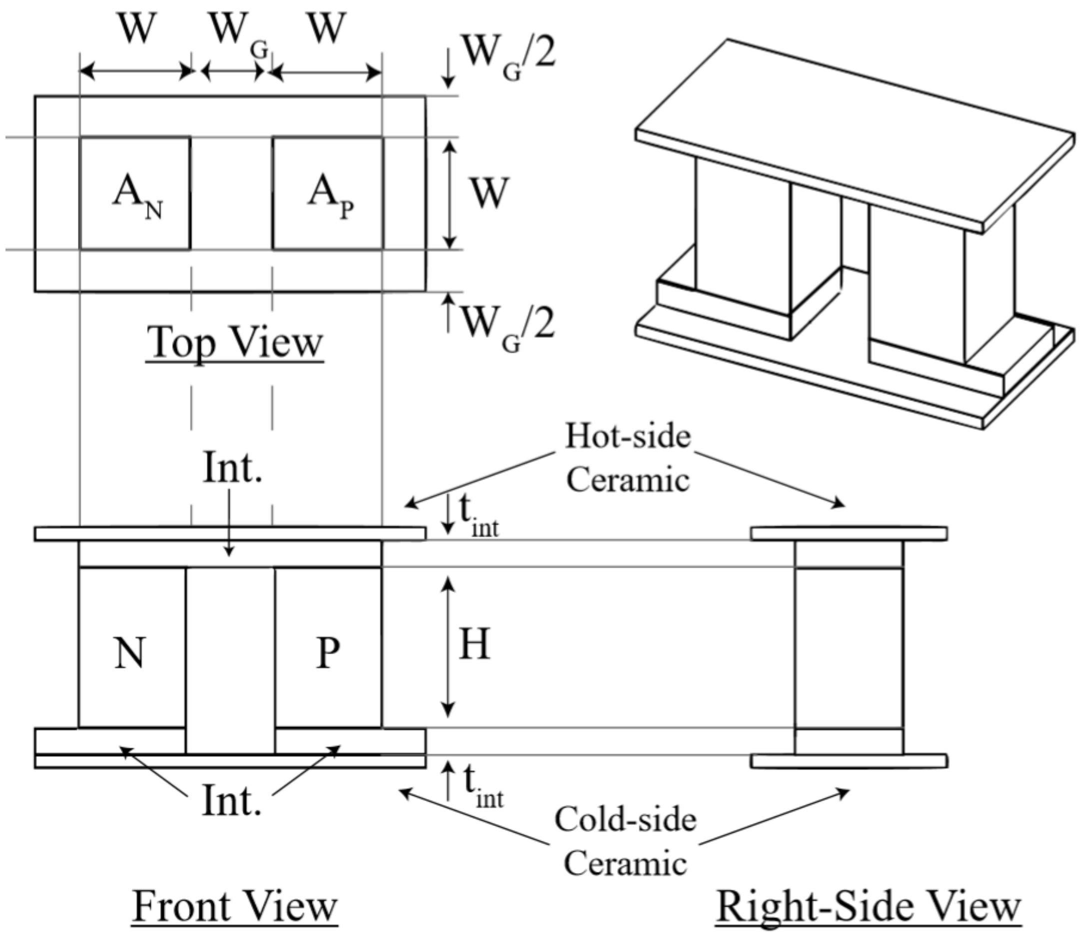

Background: TEG performance

Figure of merit for TE materials ($Z\bar{T}$):

$$Z\bar{T} = \frac{\alpha^2 \sigma_{el}}{K} \bar{T}$$

- α : seebeck coefficient
- σ_{el} : electrical conductivity
- K : thermal conductivity
- $\bar{T}$: mean temperature

Performance rests upon optimizing temperature-dependent material properties and device design

Radiative heat transfer proportional to T^4

- Minimize parasitic radiative transfer across the junction

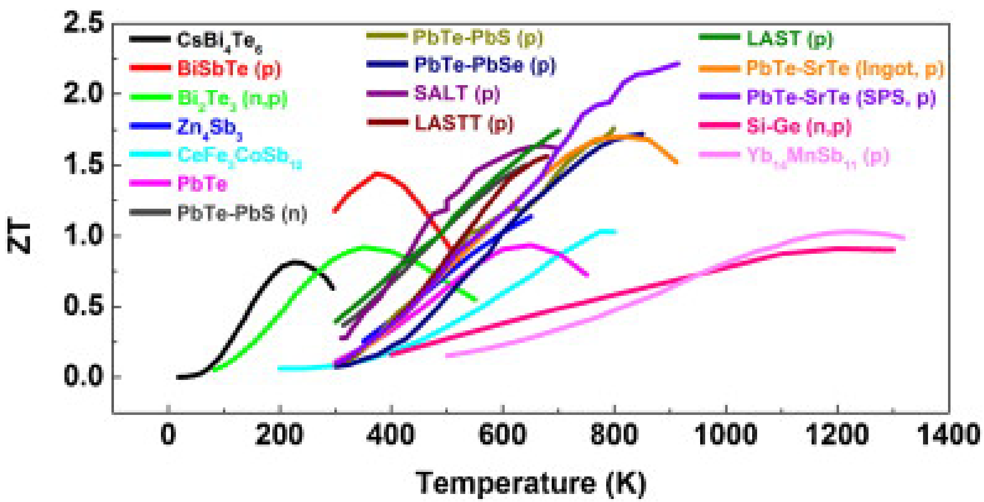

"High performance bulk thermoelectrics via a panoscopic approach" (2013) in Materials Today

Motivation: View factor

Radiation view factor (F_{ij}):

$$F_{ij} = \frac{1}{A_i} \int \int \frac{\cos\theta_i \cos\theta_j}{\pi \vec{R}^2} dA_i A_j$$

A geometric property that quantifies the proportion of diffuse radiation emitted from one surface, A_i, and received by another surface, A_j

Radiation Heat Transfer Rate (Q_i):

$$Q_i = \varepsilon \sigma A_i F_{ij} \left(T_i{}^4 - T_j{}^4\right)$$

ε : material emissivity
σ: Stefan-Boltzmann constant
T_i: temperature of emitter
T_j: temperature of receiver

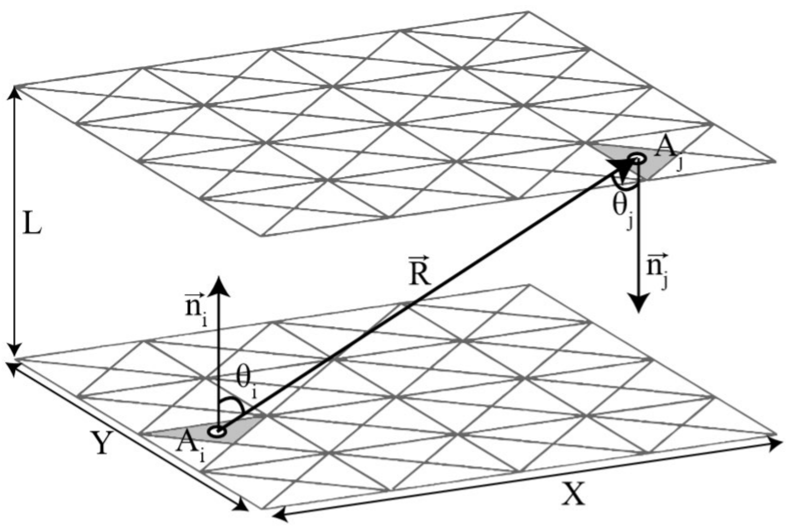

Why do we care?

Accurate heat transfer models

Parasitic radiative transfer that lowers temperature gradient

Methodology: GPU-accelerated programming and geometry definition

Graphics Processing Unit (GPU) can achieve massive runtime gains

- Thousands of cores that operate in parallel
- Computational structure is ideal for repetitive, algebraic tasks

Geometry Input: STL Files

- Ubiquitous in CAD software
- Robust geometry definition

```
solid ThermoelectricGenerator.STL
   facet normal 0.000000e+00 -1.000000e+00 0.000000e+00
      outer loop
         vertex -4.128709e-01 1.750000e+00 5.000000e-01
         vertex -4.128709e-01 1.750000e+00 -5.000000e-01
         vertex 4.128709e-01 1.750000e+00 5.000000e-01
      endloop
   endfacet
```

Example STL format

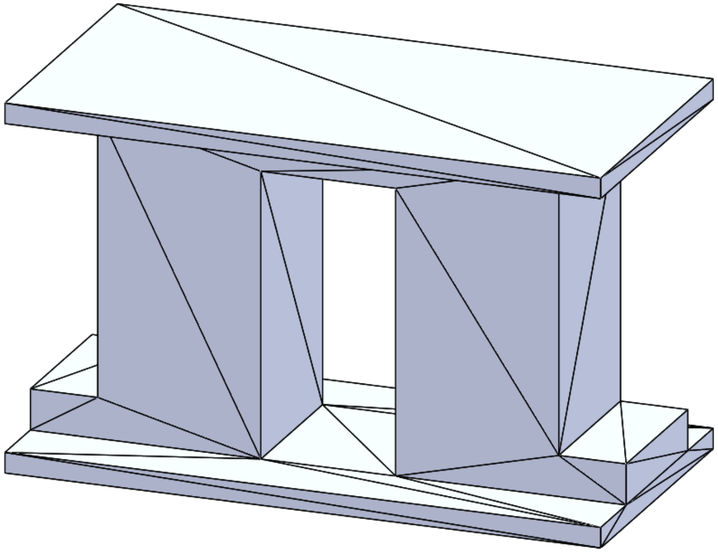

Example TEG unit-cell defined in STL format

Methodology: View factor computation

View factor: $$F_{ij} = \frac{1}{A_i}\int\int \frac{\cos\theta_i \cos\theta_j}{\pi \vec{R}^2} dA_i A_j$$

View factor summation: $$F_{ij} = \frac{1}{A_i}\sum_{i=1}^{N_i}\sum_{j=1}^{N_j} \frac{\cos\theta_i \cos\theta_j}{\pi \vec{R}^2} dA_i A_j$$

Every differential area of the emitter surface creates a corresponding ray for each receiver differential area, where the ray vectors are determined by the centroidal locations of each triangle, as determined from the STL file.

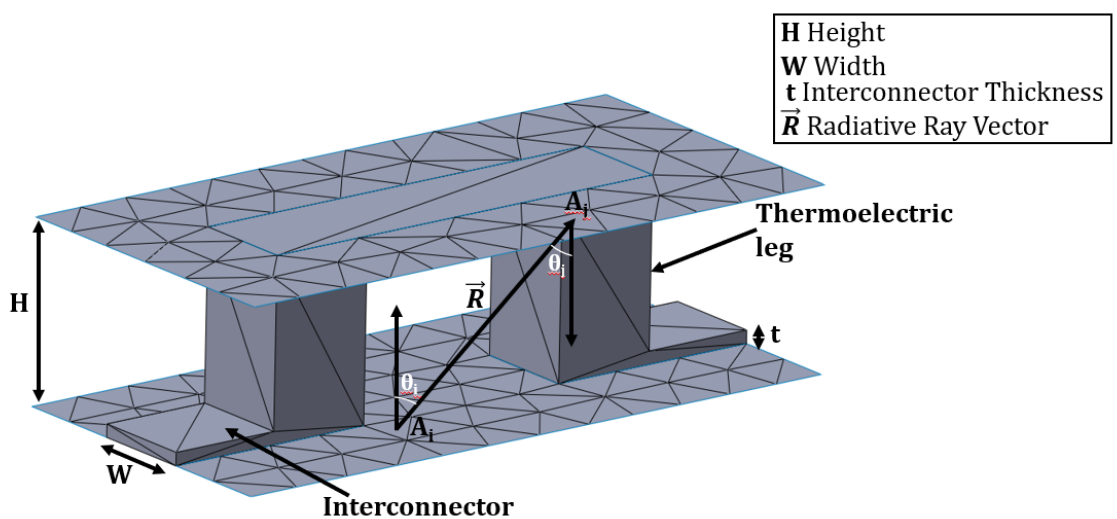

Methodology: Shadow effect and Möller–Trumbore intersection algorithm

Shadow effect: a phenomenon that represents any potential ray intersection with a non-participating surface

Reduces view factor magnitude

Möller–Trumbore ray-triangle intersection algorithm:

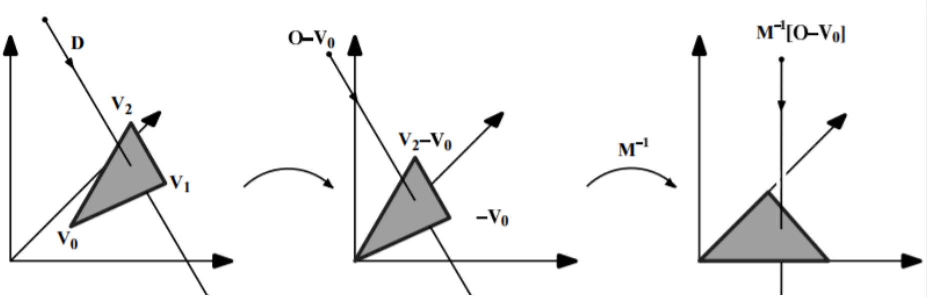

"Fast, minimum storage ray-triangle intersection" (1997) in Journal of graphics tools

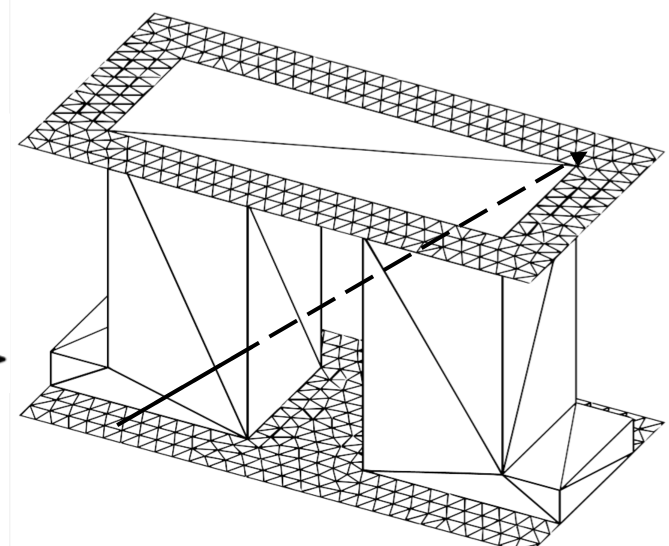

Example of shadow effect

Outline:

Methodology: Flow chart

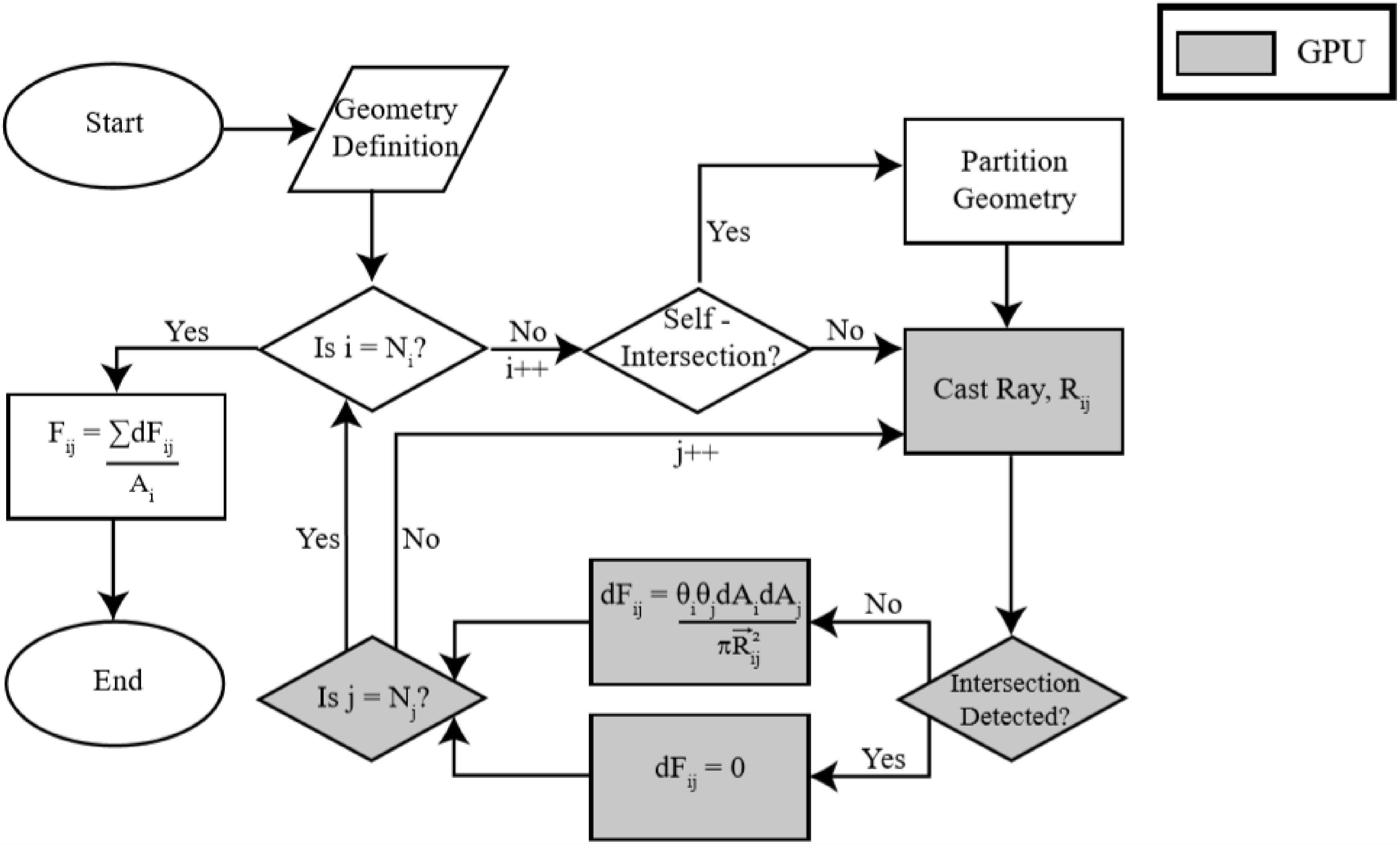

Methodology: Self-intersection

Self-intersection : refers to any obstructive surface, intrinsic of either emitting or receiving surface, that need checked by the MT algorithm for possible ray-intersection to properly resolve the view factor

Normally exhibited in curved surfaces

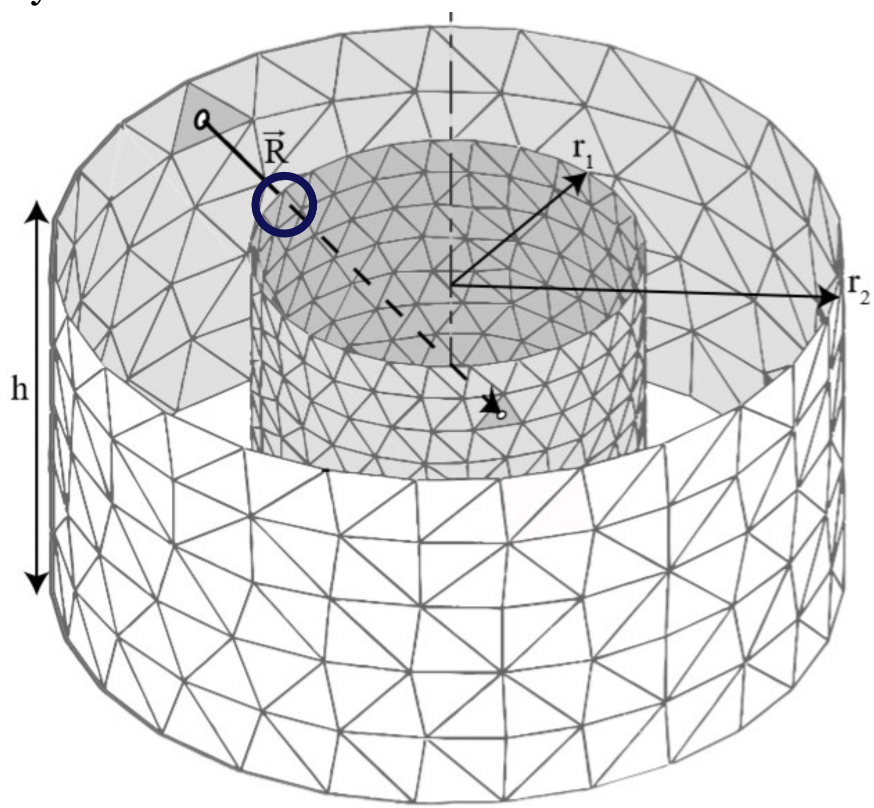

Concentric cylinders that exhibit self-intersection

Methodology: Self-intersection algorithm

Self-intersection algorithm: dynamics updates the emitting/receiving surfaces to consider only one tessellation at a time

All other surfaces are considered non-participatory (blocking)

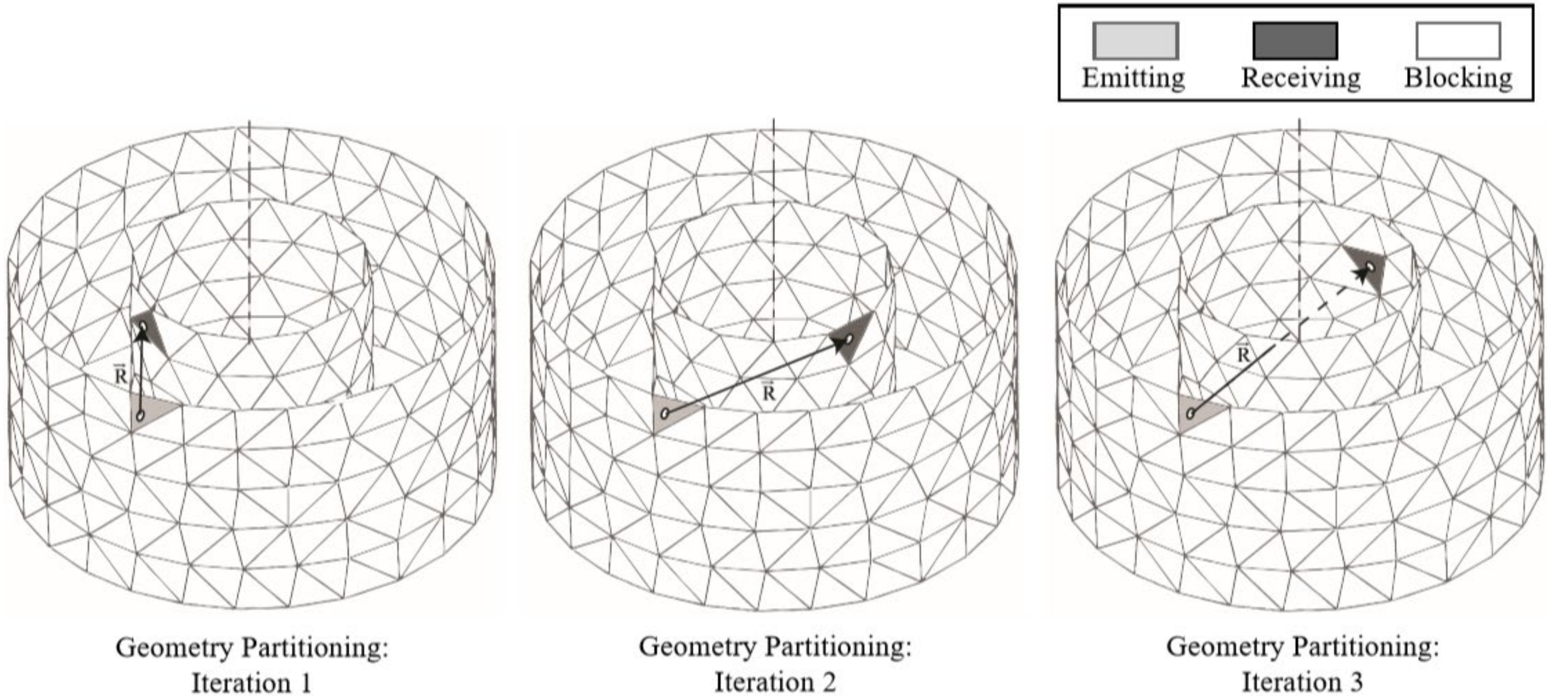

Dynamic geometry partitioning during self-intersection algorithm

Methodology: Back-face culling

Back-face culling: a computer graphics technique that refers to the removal of primitive geometries that face away from the camera

In this context, tessellations that “face away” from the emitting tessellation appear clockwise oriented

Increases computational savings and it prevents intersection miscalculations.

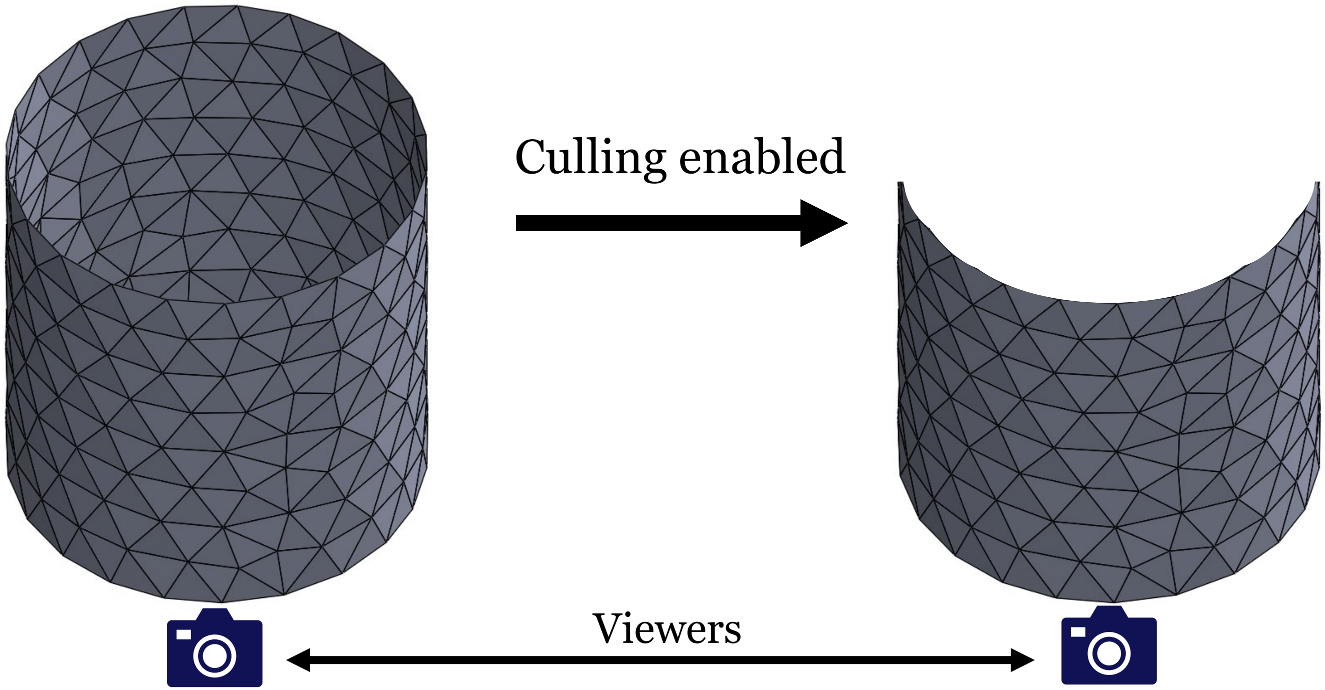

Outline:

Validation: Analytical studies

To validate the program's effectiveness, numerous geometries with published analytical solutions were inputted and tested

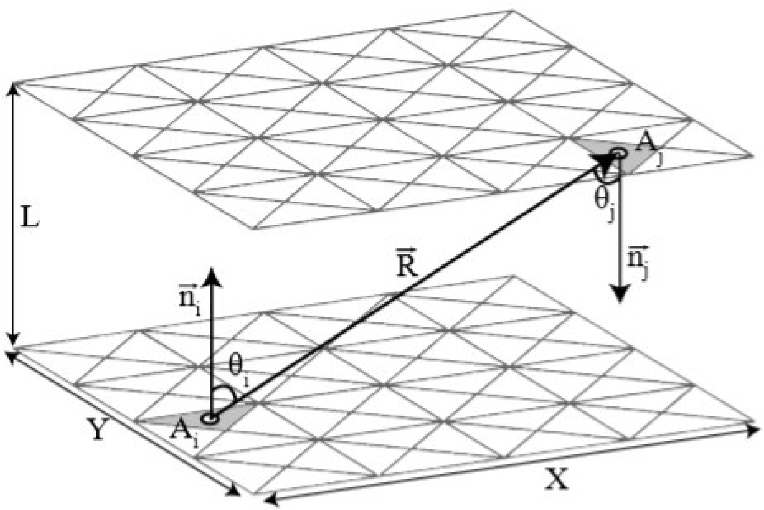

Parallel plates geometry
X/L = Y/L = 1.0

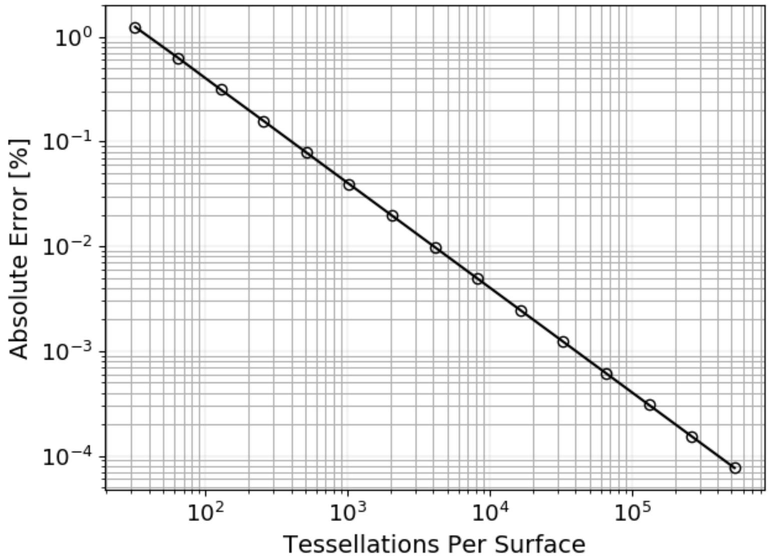

Spatial convergence with increasing mesh density

Validation: Analytical studies

More analytical test cases . . .

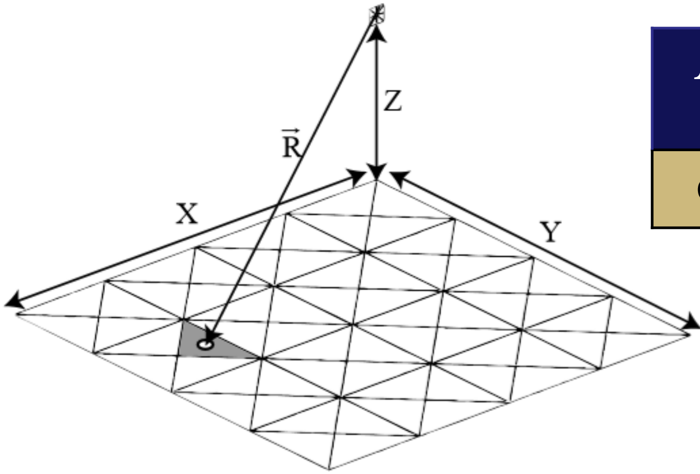

Analytical Soln.	Numerical Soln.	Percent Error
0.05573419	0.05573420	7.05725E-06

Analytical vs. numerical solutions for
Z/X = 1.0, Y/X = 1.0

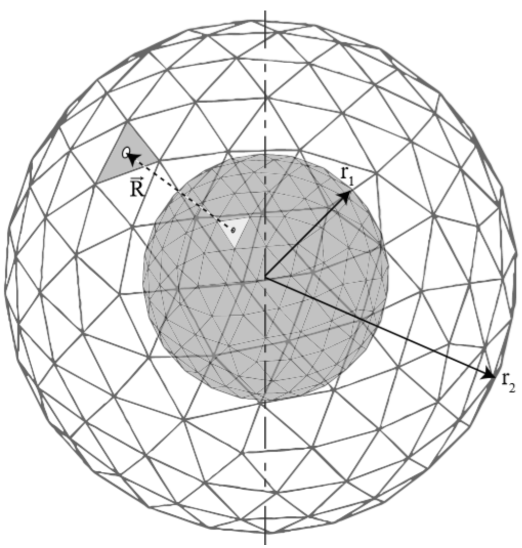

Analytical Soln.	Numerical Soln.	Percent Error
1.00	0.9988312	0.116872

Analytical vs. numerical solutions for
r1 = 0.5 [mm], r2 = 1.0 [mm]

Note: MT, self-intersection, and culling are implemented in concentric spheres

Results: Single-junction TEG

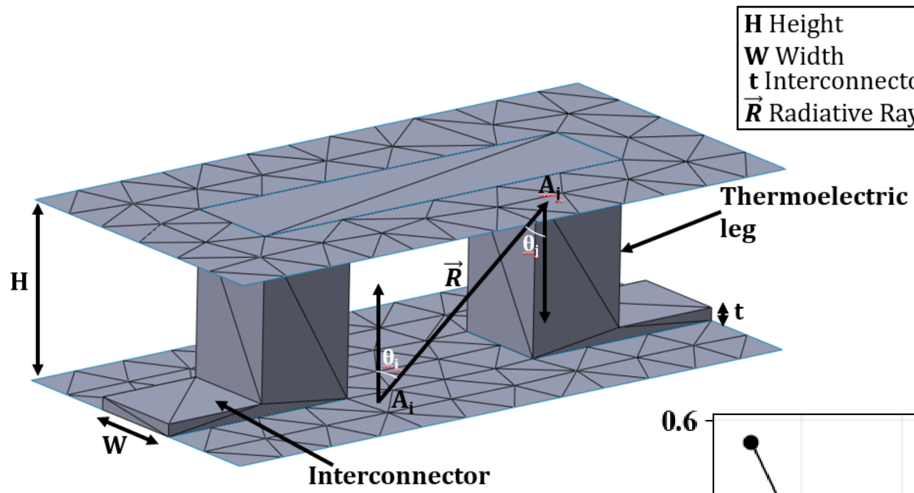

Geometrical set-up

$$\theta = \frac{N * A_P A_N}{A_{total}}$$

A_P: Area of p-type TE leg
A_N: Area of n-type TE leg
N: Number of junctions

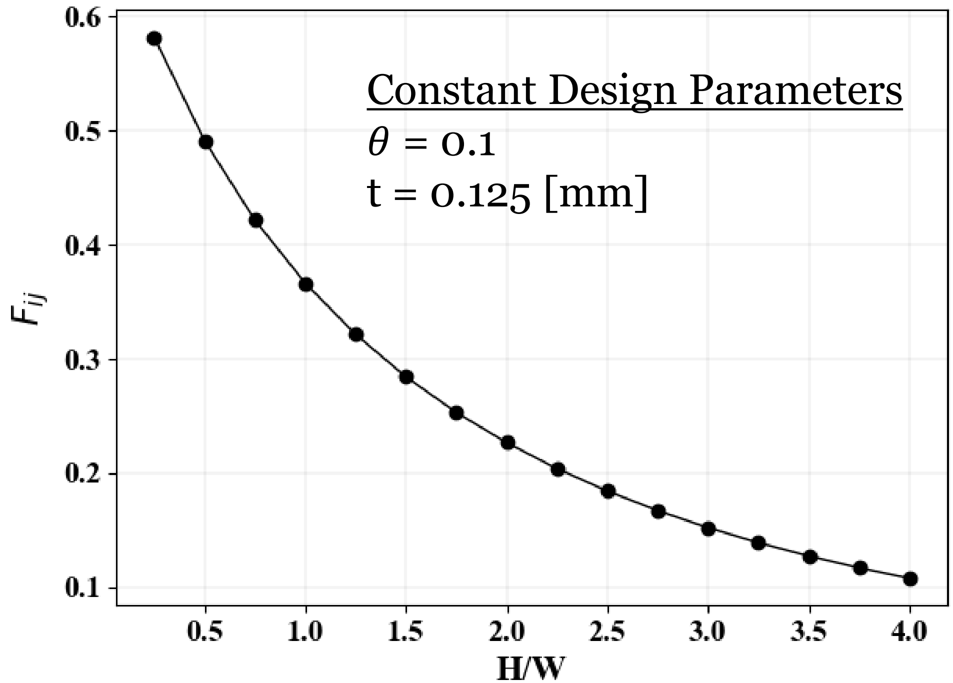

As demonstrated, the view factor decreases as H/W increases (with a constant interconnector thickness)

Due to increased prevalence of shadow effect

Results: Multi-junction TEG, H/W=0.25

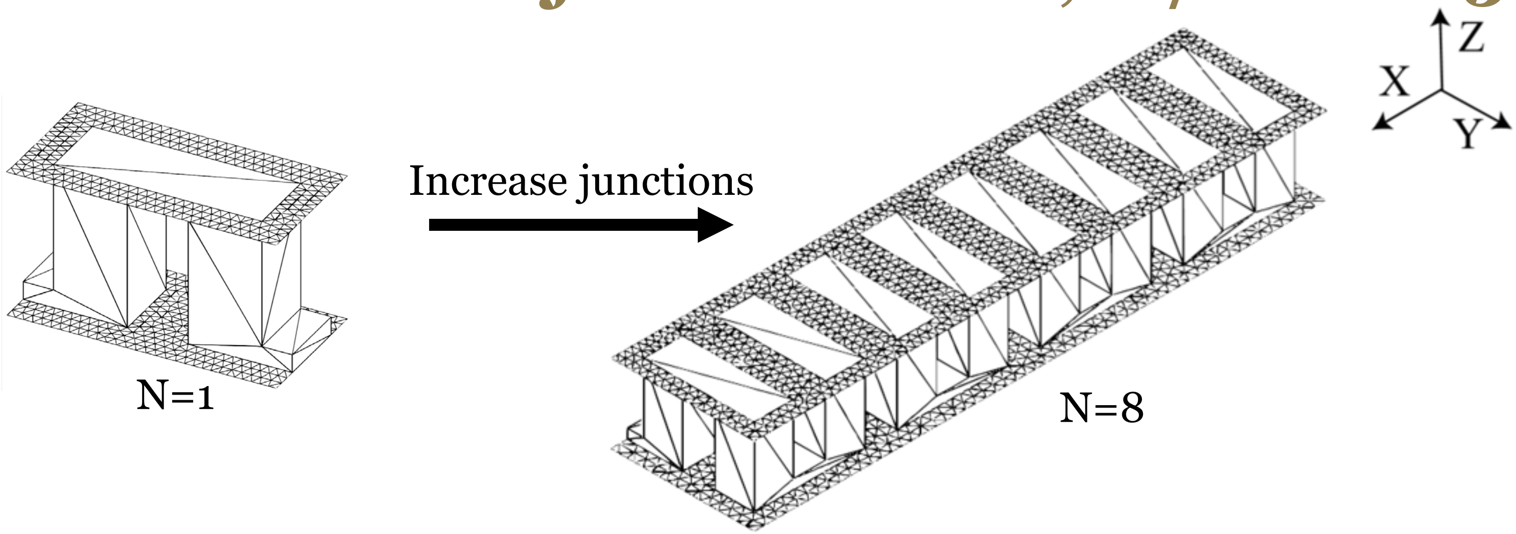

Asymptotic behavior observed in the view factor

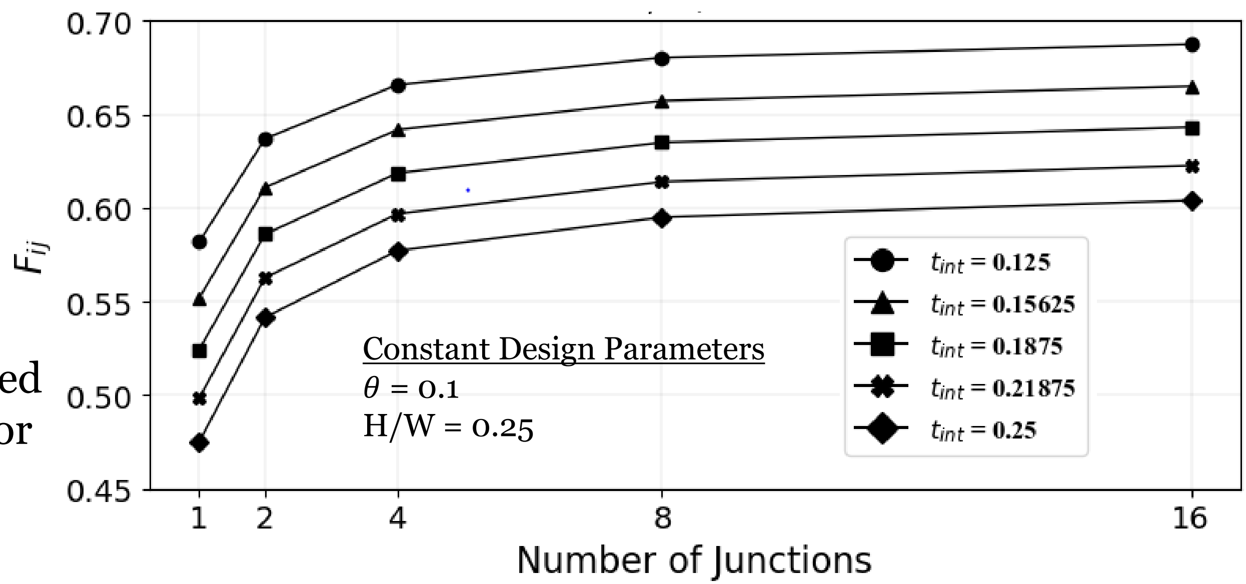

Outline:

Results: Multi-junction TEG, H/W=4.00

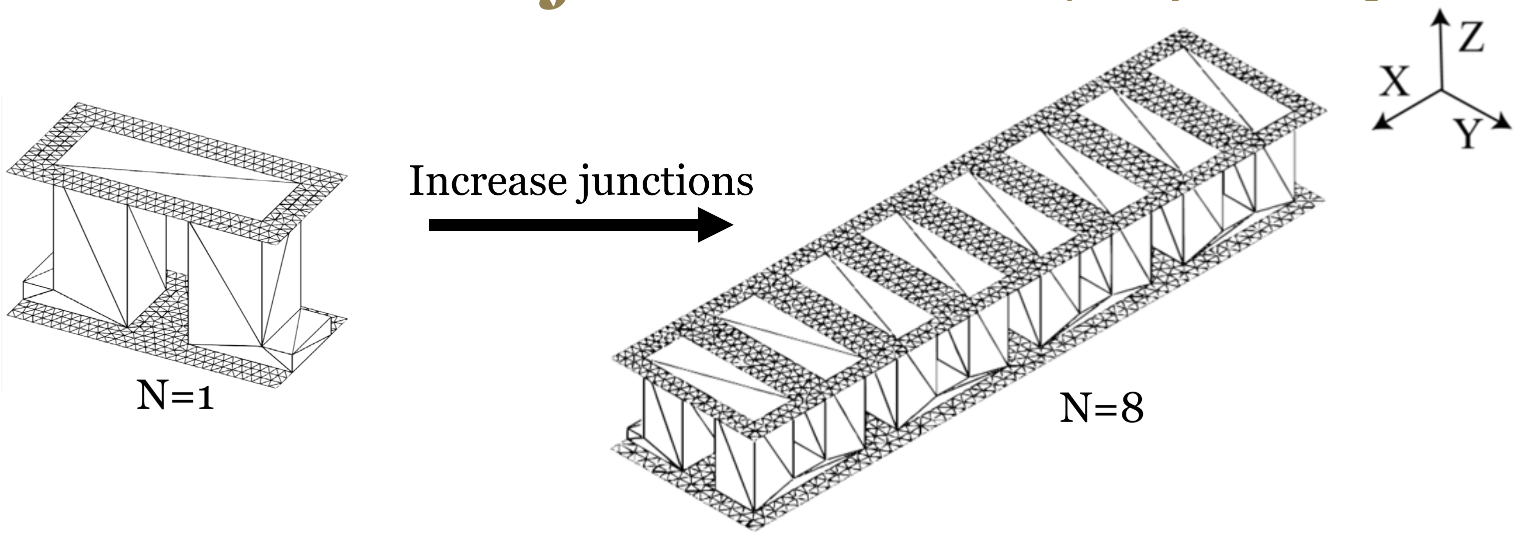

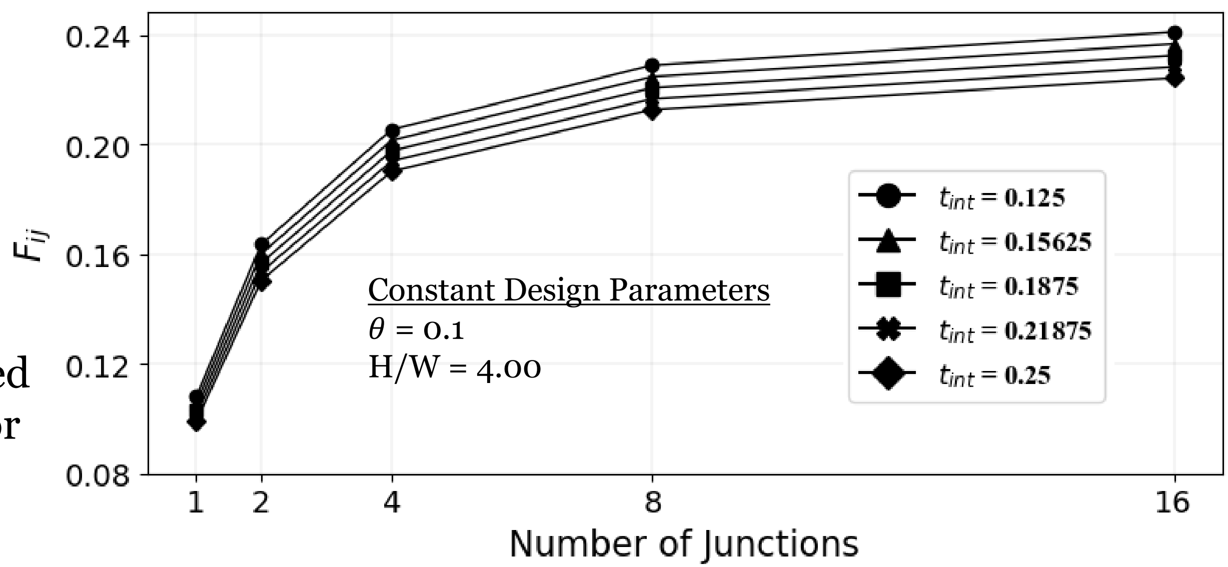

Asymptotic behavior observed in the view factor

Discussion: TEG modeling implications

Asymptotic curve demonstrates that a realistic model (N>128) could be modeled with a simpler model (N = 16)

Number of Junctions	View Factor	Absolute Difference
1	0.58177071	
2	0.637026446	0.055256
4	0.665832591	0.028806
8	0.680281868	0.014449
16	0.68751517	0.007233
128	0.694024679	0.00651

View factor values for various junction sizes: θ = 0.1 H/W = 0.25, t = 0.125 [mm].

View Factor: N = 16	View Factor: N = 128	Percent Difference
0.68751517	0.69402468	0.942356%

Percent difference between a 16 junction TEG and a 128 junction TEG

Discussion: Computational Speedup

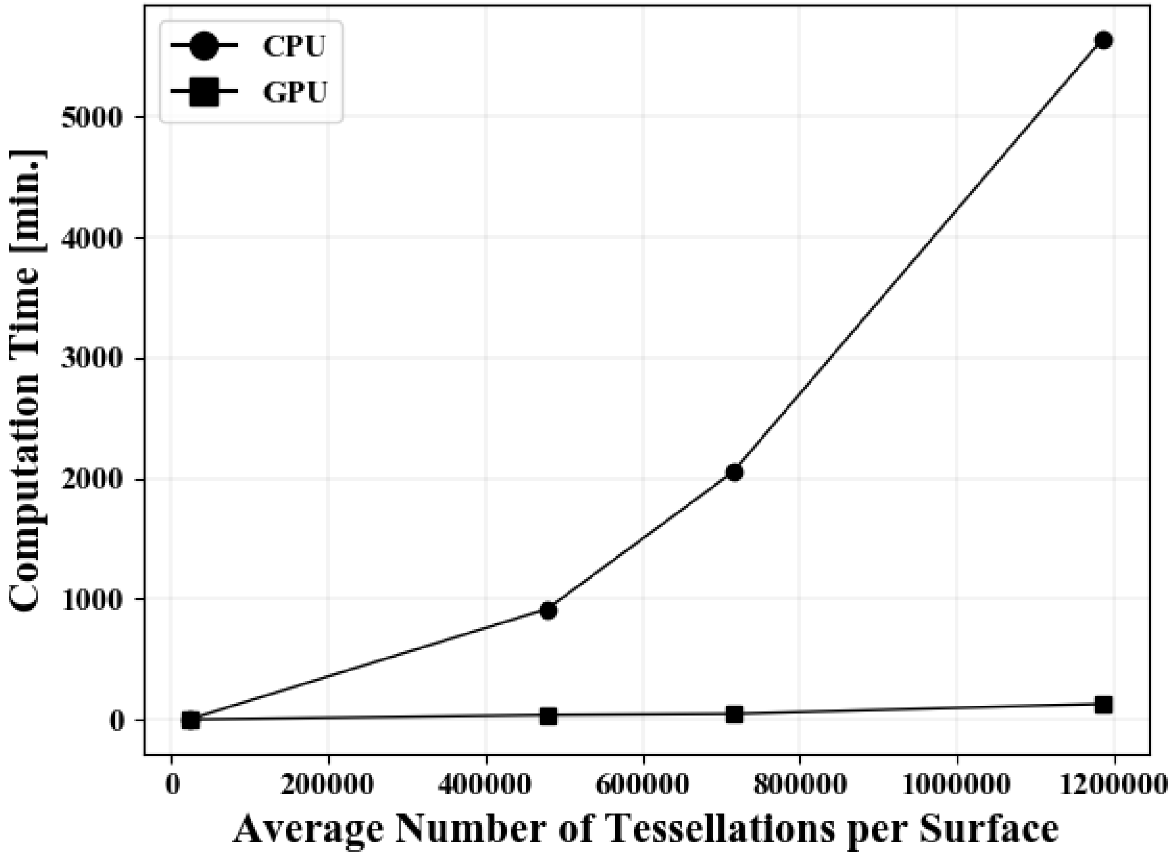

Computational time comparison between the CPU (i9-9980XE) and GPU (i9-9980XE + 2080TI) for a single-junction TEG with θ = 0.1, H/W = 0.25, t = 0.125 [mm]

GPU-acceleration becomes increasingly important as junction size grows

Conclusion

GPU-accelerated programming allows for a robust view factor calculator

- Shadow effect: MT algorithm
- Curved surfaces: self-intersection algorithm, culling enabled

As distance across a TEG hot- and cold-sides increases, the view factor decreases

For constant design parameters, as junction number increases, the view factor behaves asymptotically

- Can estimate a large and complex models with simpler models

This methodology facilitates the ability the design and analysis of high-temperature TEGs.

Acknowledgements:

Computational resources provided by the Center for Research Computing (CRC) at the University of Pittsburgh